Unraveling the Charge Distribution at the Metal-Electrolyte Interface Coupling in Situ Surface Resonant X-Ray Diffraction with Ab Initio Calculations

Y. Soldo, Eric Sibert, Maurizio de Santis, Yves Joly, Yvonne Gründer

Unravelling the charge distribution at the metal-electrolyte interface coupling *in situ* surface resonant X-Ray diffraction with *ab initio* calculations

Yvonne Soldo-Olivier, Eric Sibert[#], Maurizio De Santis, Yves Joly and Yvonne Gründer[§]*

CNRS, Université Grenoble Alpes, Institut Néel, 38042 Grenoble, France

Keywords: charge at the electrochemical interface, *in situ* Surface Resonant XRD, *ab initio* calculations, DFT, platinum single crystal

ABSTRACT

The comprehension of the mechanisms underlying the charge distribution at the electrochemical interface is a fundamental step in sight of the performing of catalytic materials. Several techniques allow the atomic structure of the metal surface to be characterized, while no experimental method allows obtaining the charge distribution of the catalyst surface and in the electrolyte in the interfacial region. Combining experimental and *ab initio* calculations, we succeeded in quantitatively describing the charge distribution at the electrochemical interface of the archetypal system Pt(111) in acidic medium. In our approach, we couple *in situ* Surface Resonant X-Ray diffraction, a site sensitive experimental technique probing both the atomic

and the electronic surface structure, with *ab initio* calculations, recently implemented to describe the Helmholtz double layer formed at the metal-solution interface. In the potential region in between the hydrogen desorption and the (bi)sulfate adsorption, we could determine the charge distribution on each of the metal surface layers and the distance separating the metal from the oppositely charged disordered ionic plane. We could reveal the presence of an electric dipole over the two outermost platinum layers. Our results demonstrate the potential of this original approach to unveil the electronic densities at the electrochemical interfaces, a challenging topic for the understanding of the electrochemical reactivity.

INTRODUCTION

In electrocatalysis, reactivities and performances are crucially affected by the atomic and electronic structure of the electrode surface and of the electrolyte forming the electrochemical interface, as well as by their stability and by the charge transfer mechanisms.

Due to the high complexity of industrial catalysts, the study of model systems has been proven to be of great help in the comprehension of such systems. In this context, single crystal surfaces have been extensively investigated, due to their ordered and well-defined structure, allowing major improvements in the comprehension of fundamental surface phenomena[1].

The atomic structure of the single crystal electrode surface and of adsorbed species has been widely explored *in situ* and *operando* with several techniques, such as Scanning

Tunneling Microscopy[2], X-ray Absorption Spectroscopy[3] and Surface X-Ray Diffraction[4,5] and enabled an atomic/molecular-level understanding of the interface.

Nevertheless, the knowledge of the charge spatial distribution at the interface as a function of the applied potential is mandatory for a complete description of the parameters influencing the electrochemical reactivity[6]. Indeed, the sign and the extent of the interfacial charge largely impact the interactions of the molecules and ions with the electrode surface.

An experimental technique able to make this description was up to now lacking. *Operando* XAS and more recently X-ray Photoelectron Spectroscopy in ambient environment[7] at the solid/liquid interface give access to the oxidation/reduction state of the surface atoms. Nevertheless, these methods do not allow a specific site selection: isolating the signal of the interface only can be difficult, all the more if the absorbing atoms are also present in the solution. Electrochemical voltammetry allows to access the total surface charge (which includes the charges due to adsorption processes). It is though the free charge[8], charge in excess on the metal surface balanced by ions in the electrolyte, which is related to the main properties of the electrochemical interface and in particular to the catalytic activity. Total and free charge coincide in absence of specific adsorption, otherwise the free charge value can only be estimated within models using extra-thermodynamic assumptions[9,10]. Resonant Surface X-Ray Diffraction (SRXRD) combines the desired properties of surface X-Ray diffraction on the site sensitivity and of X-Ray Absorption Near Edge Spectroscopy (XANES) on the atomic oxidation states. Indeed, experiments have shown a strong dependence of the recorded spectra on the potential value[11,12]. Nevertheless, up to now, the rare *ab initio* calculations[13], not considering the non-equivalent atoms, the non-zero momentum transfers and the effect of the applied electric field, resulted in a qualitative description of the surface properties.

We succeeded here in measuring for the first time the spatial charge distribution at the electrochemical interface of the archetypal system Pt(111) in acidic solution, for which the surface charge influence on common electrochemical reactions is well known[9].

This result could be achieved analyzing *in situ* surface resonant x-ray diffraction experiments by comparison with first principle simulations of the recorded spectra. These ones, while going beyond the limitations evoked above, have been recently developed to take into account for the disordered ionic plane which forms close to the charged metallic surface, following the Helmholtz model.

EXPERIMENTAL METHODS

Experiments were made at the bending magnet D2AM French CRG beamline at the European Synchrotron Radiation Facility (ESRF, France). X-ray photon energy was selected by a two crystal Si(111) monochromator with an energy resolution of about 1.5 eV in the energy interval of the spectrum, between 11520 and 11560 eV across the Pt L_{III} edge.

SRXRD was collected using a five-circle diffractometer. This set-up allows for selecting a given (HKL) reflection of the crystal with additional constraints like e.g. a fixed incidence angle, and to switch between σ and π polarization.

The sample, a platinum (111) single crystal, was placed in a home-made electrochemical cell specifically dedicated to *in situ* diffraction experiments[14]. The details of the surface preparation made before each experiment, allowing to get a clean and well-oriented platinum surface, and of the crystal transfer to the cell are given in S.I.1.

During the experiment the working electrode potential was maintained at 0.35 V_{RHE}, in the potential region in between the hydrogen desorption and the (bi)sulfate adsorption, where no adsorbed ions are expected on the Pt surface[15].

Spectra were recorded *in situ* at several positions in reciprocal space, indexed in the surface hexagonal unit cell. Diffraction from a truncated crystal shows a sharp scattering line-shaped for the momentum transfer parallel to the surface at integer (HK), and a continuous distribution as a function of L in-between Bragg peaks for momentum transfer in the out-of-plane direction. This intensity distribution is known as (HK) crystal truncation rod (CTR)[16].

Data were registered in the reflectivity geometry at the (0 0 1.5) node, sensitive only to out-of-plane order, and along the (01) crystal truncation rod (L=0.5, 1.3 and 1.8) , sensitive to both in and out-of plane order. For Pt(111), the two reflections at (0 1 0.5) and (0 0 1.5) correspond to the so-called anti-Bragg positions and are the most sensitive to the surface contributions. Experiments were made in two different configurations, corresponding to the incident beam polarization parallel (σ) to the surface plane and nearly perpendicular to it (π), probing the atomic bonds in the corresponding directions. The schematic experimental setup is schematically described in figure 1.

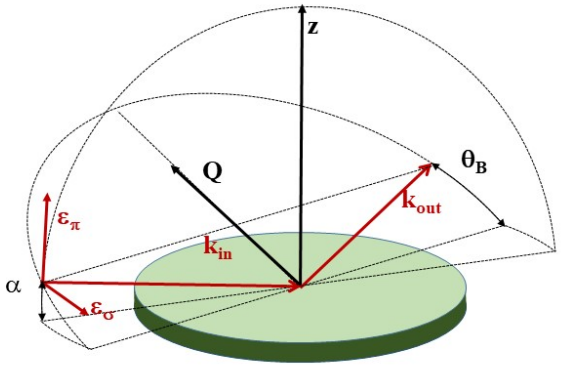

Figure 1. Scheme of the experimental geometry for the non-specular (0 1 L) reflections, collected in grazing incidence angle (α=1°). Two operating modes corresponds to incoming polarization parallel ($\boldsymbol{\varepsilon_\sigma}$) or nearly perpendicular ($\boldsymbol{\varepsilon_\pi}$) to the sample surface (incident beam electric field in the surface plane and forming an angle of 90°-α with it, respectively). z is the direction normal to the surface. The diffraction plane is also shown: it contains the diffraction vector **Q**, and the incoming ($\mathbf{k_{in}}$) and outgoing ($\mathbf{k_{out}}$) wave vectors. θ_B is the Bragg angle.

The fluorescent signal emitted by the sample was simultaneously recorded using a photomultiplier with NaI scintillator: absorption Pt_{LIII} edge position was used as energy calibration, allowing the comparison among the spectra.

Between the sample and the diffracted beam detection, we installed a Panasonic R90 graphite crystal analyzer, to reject the spurious diffused photons and the fluorescence signal and ensure that only elastically diffused photons are detected. Diffracted beam was recorded by a bidimensional pixel photon counting detector IMXPAD S70: measured intensity at each energy corresponds to the integrated signal recorded on a previously defined region of interest.

Details on the measurement operation mode and on the correction and normalization procedures applied to the experimental spectra are given in S.I.2.

Crystal truncation rod (0 1 L) was also measured at fixed energy for structural analysis. The surface structure obtained from the best fitting procedure, in excellent agreement with previous *in situ* SXRD measurements on Pt(111) in 0.05M H_2S0_4 in the same potential region, has been used in the simulation procedure. Details are given in S.I.3. Using the conventional hexagonal unit cell for the (111) surface, with the c axis perpendicular to the crystal surface[17], the Pt(111) surface is described by four atomic layers, positioned above the bulk substrate taken as the platinum semi-infinite crystal. The first three planes are fully occupied with an interplanar distance equal to the bulk one (2.265 Å), while the outermost layer is partially occupied (0.96) and the interlayer distance is expanded by 1.5% (2.30 Å).

THEORETICAL CALCULATIONS

Calculations were performed using the FDMNES[18,19] software, which uses the Density Functional Theory. The self-consistent approach is explained in the reference. Recently extended for the simulation of surface resonant diffraction experiments[20], it has now been developed for the electrochemical interface description, to take into account for the presence of the electrolyte facing the crystal and the effect of the applied external electric field.

When a (charged) metal is in contact with a liquid, a charge exchange happens between the two phases due to the initial gradient of the electrochemical potential[21]. Following this mechanism, the simplest model to describe this phenomenon was proposed by Hermann von Helmholtz. It states that a double layer of opposite polarity forms at the electrochemical interface[22]. In absence of specific adsorption, the interfacial double layer is described by the plane of the metal

surface and by the plane containing the counter ions[23]. At the potential of zero charge (pzc), the charge located at the interface vanishes.[24].

In this context, FDMNES can model the electrochemical interface adding a potential V(z) (z coordinate perpendicular to the crystal surface) to the surface atomic structure potential. This additional potential simulates the presence of a non-ordered ionic layer (Helmholtz outer plane) at a distance z_0 from the top most surface atomic plane.

Given the position z_0, the FWHM Δ_V, and the amplitude V_0, the Helmholtz layer is modelled by the energy potential:

$$V(z) = \frac{\sqrt{\pi}}{2} V_0 \frac{\mathrm{erf}(\frac{z - z_0}{\alpha \Delta_V})}{\frac{z - z_0}{\alpha \Delta_V}} \qquad Eq.1$$

with α=0.285925223. A negative V_0 energy value corresponds to a positive ionic layer. This potential is simply added to the potential resulting from the surface atomic structure.

Figure 2 gives a schematic representation of the potential visualizing the different parameters used in the simulations.

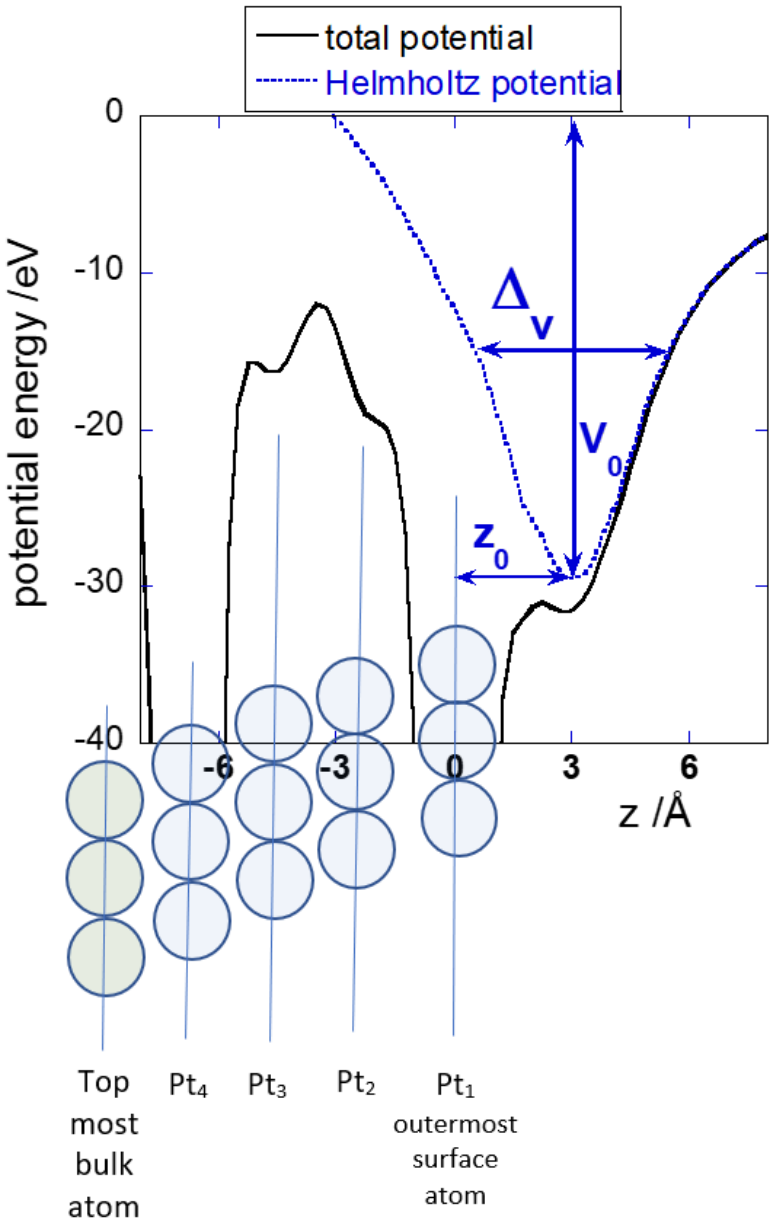

Figure 2. Total potential (continuous black line) as a function of the z coordinate perpendicular to the crystal surface through the outermost surface atom Pt_1 (z=0); Helmholtz contribution (V_0=-30 eV, z_0=3 Å, Δ_V=5 Å) is represented by the blue dotted line. Schematic representation of the Pt surface structure is overlapped.

The formula (Eq. 1) being partly empirical, the relationship between V_0 and the charge in the Helmholtz layer is not known. They must nevertheless be proportional between them and thus also proportional to the induced charge at the surface.

Calculations were performed as a function of the parameters V_0 and z_0, the distance between the Helmholtz layer and the surface. The ΔV parameter, poorly sensitive, has been set equal to 5Å, this large value taking into account for the disordered nature of the Helmholtz ionic plane. One of the effects of the Helmholtz layer being to induce a total charge Ch per Pt atom in the top most surface layers, this last is also a parameter. The self-consistent procedure makes that it is shared between the different top most layers, Ch_i representing the charge per atom on each surface layer i. Further technical details are given in the S.I. 4.

In the present study we have neglected the non-resonant Thomson scattering of this ionic layer, eventually visible in any case only at the specular reflections [25]. Indeed, its effect is expected to affect the experimental intensity by less than a few percent, due to the very high Pt scattering amplitude and to the structural disorder of the plane also in the perpendicular direction. This layer has nevertheless an influence on the electronic structure of the surface atoms, in particular inducing an expansion of the last inter-reticular distance.

The comparison between simulations and data is made using the total metric distance D, as detailed in S.I. 5.

RESULTS AND DISCUSSION

Experimental data

Resonant spectra are shown in figure 3. At (0 1 1.8) along the (0 1) CTR, close to the (0 1 2) Bragg peak, the experimental data presents a very similar behaviour in the two polarizations, both for the signal shape and the fine structures beyond the edge. Such observation agrees with

the fact that at this (*HKL*) position the surface layers make only a small contribution to the total scattered intensity and the Pt bulk symmetry implies no sensitivity to the polarization[26].

The spectra evolve moving away from the Bragg peak. At L=1.3, measured only in π polarization, the signal is already largely modified. At the non-specular (0 1 0.5) and specular (0 0 1.5) anti-Bragg positions, fine structure of the spectra beyond the edge is very different in the two polarizations. We remark that the specular data in σ polarization seems to present an unexpected behavior below the edge energy.

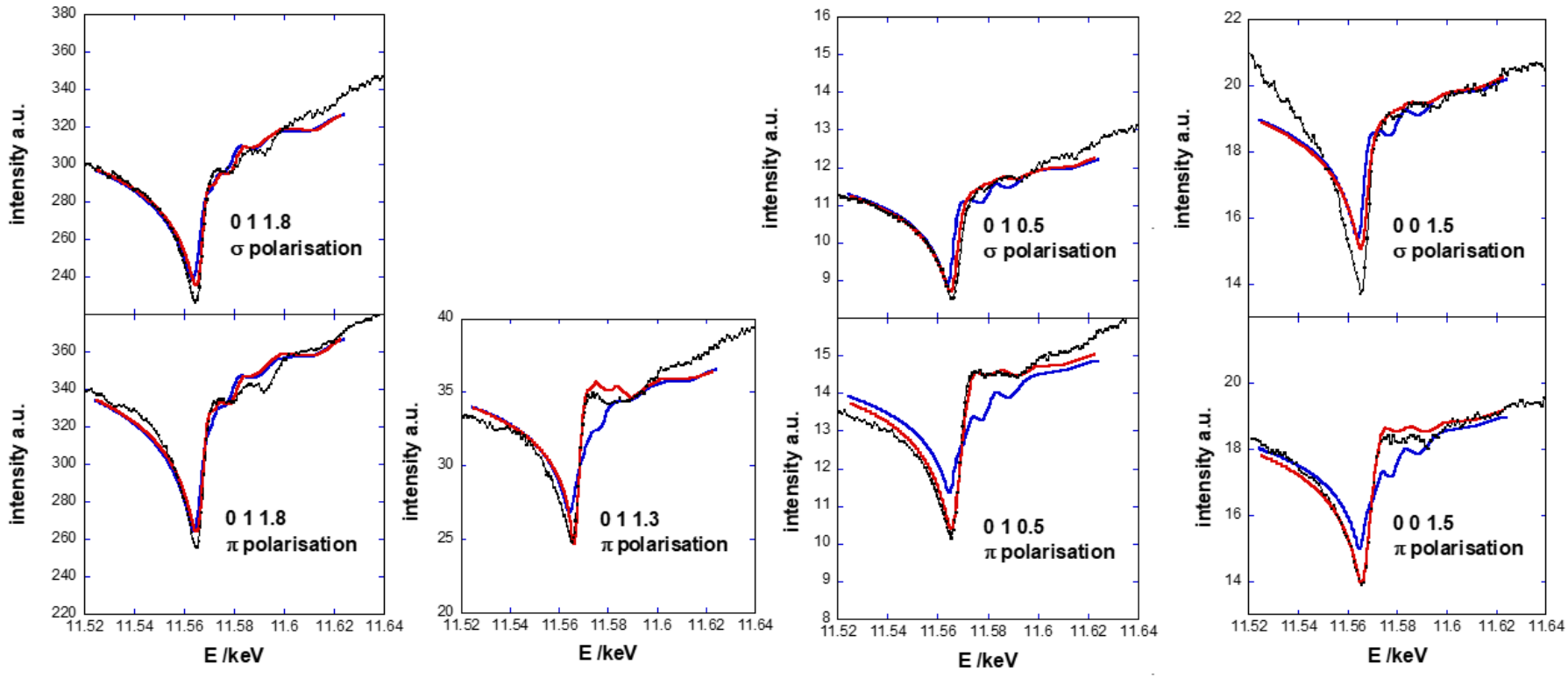

Figure 3. Normalized experimental spectra (black dots) recorded at (0 1 1.8), (0 1 1.3), (0 1 0.5) and (0 0 1.5) in σ and π polarizations and FDMNES *ab initio* calculations with (red continuous line) and without (blue continuous line) Helmholtz potential (V_0=-35 eV, z_0=3 Å, Δ_V=5 Å, surface atomic charge Ch=-0.2).

First principle simulation

As shown by the contour lines of the metric distance D, our confidence factor to compare simulation and data, D is large when $V_0 \geq 0$ (figure 4). A well-defined minimum is found in the negative energy potential region for V_0=-35±5 eV and a total negative surface charge Ch=-0.20±0.05, which corresponds to about 50 μC/cm^2 (1.5·10^{15} platinum atoms/cm^2).

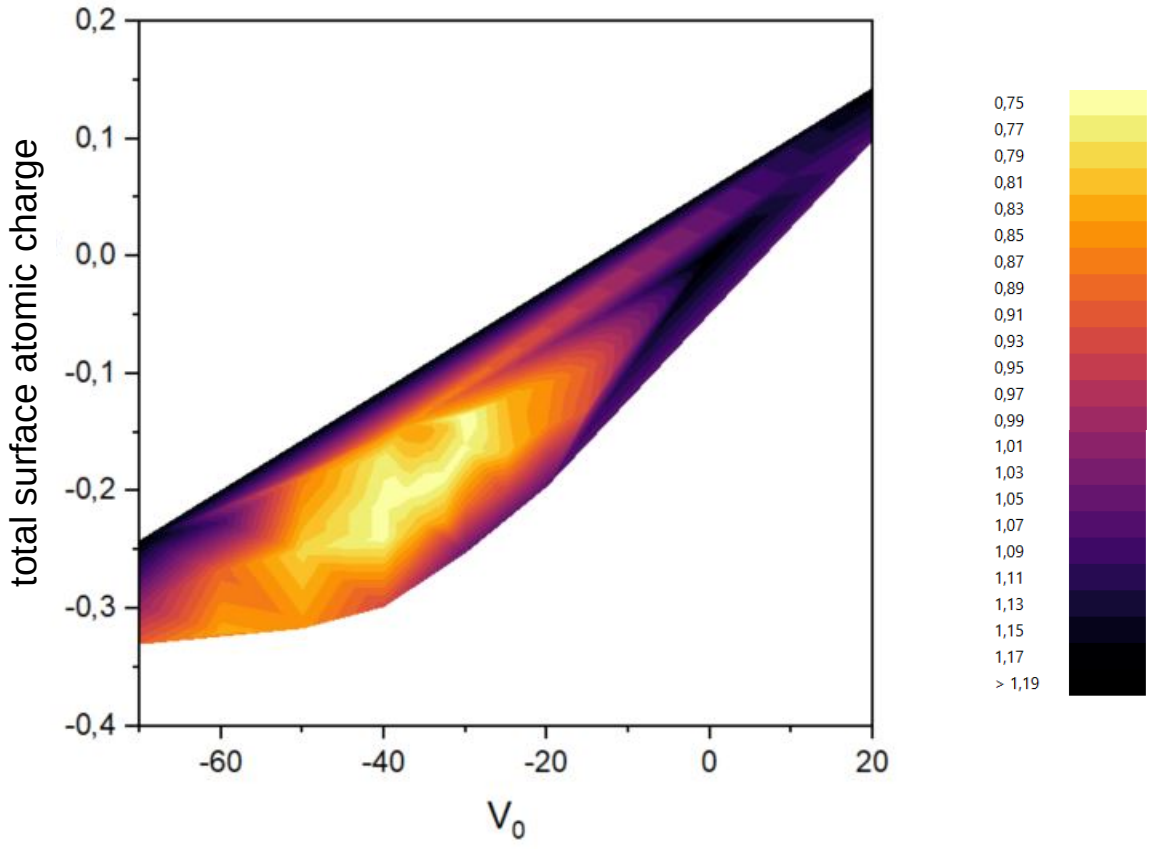

Figure 4. contour lines of the total metric distance D (given as a percentage) as a function of the V_0 value describing the Helmholtz potential and the total surface atomic charge Ch.

The corresponding position of the positive ionic plane z_0 results to be 3.1±0.5 Å. Although limited to some tenths of Ångstrom, the sensitivity is remarkable, considering that it refers to average position of a highly disordered plane.

The agreement between experiments and simulation is here remarkably good, as shown in figure 3. Both intensity and fine structure are well reproduced for all the spectra, with the only exception of the intensity in the pathological spectrum recorded at (0 0 1.5) in σ polarization. The very good matching of best simulation with data confirms that the non-resonant Thomson diffusion by the Helmholtz ionic layer and the water absorption dependence from the photon energy are negligible, as assumed in our calculations.

The expected linear correspondence between V_0 and the induced charge is verified as the best agreement with experiment follows a linear combination of these parameters, as it can be seen in figure 4.

Our calculations allow the description of the atomic charge on each surface plane. We found that the charge is not limited to the outer topmost Pt plane, but to the two topmost ones, Ch_1=-0.47±0.1, Ch_2=0.27±0.05, while the charges on the underlaying Pt_3 and Pt_4 planes are negligible, Ch_3=+0.01 and Ch_4=-0.01. Figure 5 gives a schematic representation of the charge distribution at the electrochemical interface.

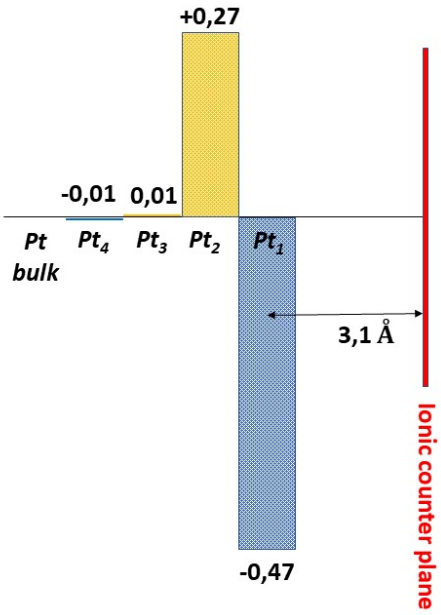

Figure 5. Schematic representation of the charge distribution, charge per platinum atom, at the electrochemical interface.

This is the first experimental observation of the presence of an electric dipole in the metal surface in absence of adsorption effects. These results support the presence of a negative capacitance for some Pt surface layers, as suggested by theoretical works to explain the presence of a peak near the pzc for the differential capacitance curve of Pt(111)[27]

The sensitivity of this technique to the surface atomic charge associated to the Helmholtz layer can be checked comparing our best result with calculations without the Helmholtz potential (Figure 3). The anti-Bragg reflections calculated with V_0=0 differ significantly from the experimental spectra. The effect is even stronger for the non-specular anti-Bragg reflection recorded with π polarization. It is indeed specifically sensitive to the electronic environment perpendicular to the surface, where the Helmholtz stands (see table 1).

	No Helmholtz D=1.19 (%)	**Helmholtz D=0.75 (%)**
D_1 (0 1 0.5) σ pol.	0.97	0.55
D_2 (0 1 0.5) π pol.	2.22	0.75
D_3 (0 1 1.3) π pol.	1.36	1.01
D_4 (0 1 1.8) σ pol.	0.73	0.63
D_5 (0 1 1.8) π pol.	0.74	0.67
D_6 (0 0 1.5) σ pol.	1.35	1.14
D_7 (0 0 1.5) π pol.	0.98	0.51

Table 1. Metric distances D_i with the FDMNES simulation calculated for each experimental spectrum without and with the Helmholtz potential (V_0=-35 eV, z_0=3 Å, Δ_V=5 Å, total atomic charge Ch=-0.20±0.05).)

Hence, even if measurements were recorded at 0.350 V_{RHE}, only some tens of mV lower than the Pt(111) pzc estimated equal to about 0.380 V_{RHE} [28, 10], our data clearly demonstrate that here the surface model free of charge is not the adequate description. Previous *ab initio* molecular dynamic

calculations already suggested that at the pzc, a partial charge transfer occurs from the solvating water layer to the Pt electrode leading to a dipolar polarization distribution along the interface normal [29].

Analyzing the influence of the best matching Helmholtz potential on the individual metric distances D_i (Table 1), the highest influence is found for the anti-Bragg signals; they are the most sensitive to surface contribution and D_i diminishes by at least a factor two. The effect is even stronger for the non-specular anti-Bragg reflection recorded with π polarization. It is indeed specifically sensitive to the electronic environment perpendicular to the surface, where the Helmholtz layer stands. The only exception is the simulation of the specular spectrum in σ polarization, where a decrease by only 15% of the metric distance D_6 is found. The Helmholtz potential still improves the reproducibility of the (0 1 1.3) spectrum in π polarization (-26% of D_3), while it has a smaller influence on the simulation of the (0 1 1.8) data (D_4 and D_5 decrease by about 10%).

As expected, due to the limited energy interval of the spectrum [30] SRXRD is more sensitive to the charge distribution of the interface than to interplanar distances (S.I.6), moreover accessible with the classical surface X-Ray Diffraction technique.

CONCLUSIONS

Charges at the electrochemical interfaces play a major role in the performances of the electrocatalysts. Their knowledge is mandatory to fully understand the reaction mechanisms, allowing the performing of more efficient electrode materials.

Our work has proven that *in situ* SRXRD coupled with *ab initio* calculations provides a new tool giving access to the surface electronic charge distribution of electrochemical interfaces.

We succeeded in quantitatively describing the interface charge distribution of the Pt(111) in 0.1M H_2SO_4 archetypal system. At 350 mV_{RHE}, close to the pzc potential value, a negative total surface atomic charge equal to -0.2±0.05 was found. This charge is actually distributed over the two last surface Pt layers, Ch_1=-0.47±0.1, Ch_2=0.27±0.05, corresponding to an electric dipole in the metal surface. We could determine the position of the positive counter ionic plane at 3.1±0.5 Å with a quite good sensitivity, despite its disordered structure.

Moreover, thanks to the site selection, this new approach will allow elucidating the partial charge transfer problem in presence of adsorbed species[31], identifying the individual element's charge (crystal surface, adsorbed molecules, electrolyte).

This method will make a valuable contribution to the up to now lacking experimental evidence of surface charge distribution, which is mandatory to validate the theoretical predictions. We believe that, beyond the here studied system, this new technique will allow an original and deeper comprehension of electrochemical processes.

Corresponding Author

Yvonne Soldo-Olivier
CNRS, Université Grenoble Alpes, Institut Néel, 38042 Grenoble, France
yvonne.soldo@neel.cnrs.fr

Author information

[#] Eric Sibert
LEPMI, Univ. Grenoble Alpes, Univ. Savoie Mont Blanc, CNRS, Grenoble INP, St. Martin d'Hères, France

[§] Yvonne Gründer
Oliver Lodge Laboratory, Department of Physics, University of Liverpool, United Kingdom

Author Contributions

Y.S.O., E.S., M.D. and Y.J. conceived the project, designed and performed experiments. Y.S.O., Y.J and Y.G. discussed the idea for modelling the data. Y.J. wrote and modified the FDMNES code for simulation of the data. Y.S.O. conducted FDMNES calculations. The manuscript was written through contributions of all authors.

Supporting Information. SI_SOLDO_SRXRD_Pt111_ACSCatalysis.docx

The electrochemical operation mode and the electrochemical cell for *in situ* SRXRD experiments are described in SI.1. The experimental procedure followed during SRXRD measurements is given in SI.2. Comparison of the fitting and the (0 1 L) CTR experimental signal is shown in figure S2 (section SI.3). The details of the *ab initio* calculations are given in SI.4. The description of the confidence factor used is detailed in SI.5. Figure S3 (section SI.6) displays the sensitivity of SRXRD spectra for the interplanar distance between the two outermost platinum surface layers.

ACKNOWLEDGMENT

Beam time at the French CRG BM2 beamline of the ESRF (Grenoble, France) is acknowledged. We thank the BM2 staff for support. Y.G. thanks the Royal Society for funding through a University Research Fellowship (URF\R\180005) and a research grant (RGF\EA\181030).

REFERENCES

[1]. Ertl, G. Reactions at surfaces: from atoms to complexity (Noble Lecture). *Angewandte Chem. Int. Ed.* **2008,** 47, 3524-3535.

[2]. Kolb, D. and Simeone, F.C. ed. Michael Bowker, P.R. Davies, *Scanning tunneling microscopy in surface science, chapter 5 : Characterization and Modification of electrode surfaces by in situ STM*, (Wiley Online Library, 2009).

[3]. Masuda, T.; Kondo, T. New sights into the electrochemical interface provided by *in situ* X-Ray absorption fine structure and surface X-Ray scattering. *Curr. Opin. Electrochem.* **2019,** 14, 81-88.

[4]. Gründer, Y.; Lucas, C.A. Surface X-ray diffraction studies of single crystal electrocatalysts. *Nano Energy* **2016,** 29, 378-393.

[5]. Nakamura, M. New insights on structural dynamics of electrochemical interface by time-resolved surface X-ray diffraction. *Curr. Opin. Electrochem.* **2019**, 14,200–205.

[6]. Schmickler, W. Electronic effects in the electric double layer. *Chem. Rev.* **1996,** 96, 3177-3200.

[7]. Savaleva, V.A.; Savinova, E. R. Insights into electrocatalysis from ambient pressure photoelectron spectroscopy. *Curr. Opin. Electrochem.* **2019,** 17, 79-89.

.[8] Martinez-Hincapié, R.; Climent, V.; Feliu, J.M. New probes to surface free charge at electrochemical interfaces with platinum electrodes. *Curr. Opin. Electrochem.* **2019,** 14, 16-22.

[9]. Briega-Martos, V.; Herrero, E.; Feliu, J. M., Pt(hkl) surface charge and reactivity. *Curr. Opin. Electrochem.* **2019**, 17, 97–105.

[10]. Rizo, R.; Sitta, E.; Herrero, E.; Climent, V.; Feliu, J. M. Towards the understanding of the interfacial pH scale at Pt(111) electrodes. *Electrochim. Acta* **2015,** 162, 138–145.

[11]. Grunder Y.; Lucas C.A. Probing the charge distribution at the electrochemical interface, *PCCP* **2017,** 19, 8416-8422.

[12].Chu, Y. S.; You, H.;, Tanzer, J. A.; Lister, T. E.; Nagy Z. Surface Resonance X-Ray Scattering Observation of Core-Electron Binding-Energy Shifts of Pt(111)-Surface Atoms during Electrochemical Oxidation. *PRL* **1999,** 83(3), 552-555.

[13]. Menzel, A.; Changa, K.-C.; Komanickya, V.; Youa, H.; Chub, Y. S.; Tolmachevc, Y. V.; Rehr. J. J. Resonance anomalous surface X-ray scattering. *Radiation Physics and Chemistry* **2006,** 75, 1651–1660.

[14]. Lebouin; C.; Soldo-Olivier, Y.; Sibert, E.; De Santis, M.; Maillard, F.; Faure, R. Evidence of substrate effect in hydrogen electroinsertion into palladium atomic layers via *in situ* surface X-Ray diffraction., *Langmuir* **2009,** 25(8), 4251–4255.

[15]. Kondo, T.; Masuda, T.; Aoki, N.; Uosaki, K. Potential-Dependent Structures and Potential-Induced Structure Changes at Pt(111) Single-Crystal Electrode/Sulfuric and Perchloric Acid Interfaces in the Potential Region between Hydrogen Underpotential Deposition and Surface Oxide Formation by In Situ Surface X-ray Scattering. *J. Phys. Chem. C* **2016,** 120, 16118−16131.

[16]. Robinson, I. K. Crystal truncation rods and surface roughness *Phys. Rev. B* **1986**, 33, 3830-3836.

[17]. Grübel, G.; Huang, K.G.; Gibbs, D.; Zehner, D.M.; Sandy, A.R.; Mochrie, S.G.J. Reconstruction of the Pt(111) surface: X-ray-scattering measurements. *Phys. Rev. B,* **1993,** 48, 18119-18139.

[18]. Bunău, O.; Joly, Y. Self-consistent aspects of x-ray absorption calculations. *J. Phys. : Condens. Matter* **2009,** 21, 345501;

[19] Bunău O.; Ramos A. Y.; Joly Y. The FDMNES code, International Tables for Crystallography, Volume I, X-ray Absorption Spectroscopy and Related Techniques, **2021**

[20]. Joly, Y.; Abisset, A.; Bailly, A.; De Santis, M.; Fettar, F.; Grenier, S.; Mannix, D.; Ramos, A. Y.; Saint-Lager, M.-C.; Soldo-Olivier, Y.; Tonnerre, J.-M.; Guda, S. A.; Gründer,Y. Journal of Chemical Theory and Computation **2018,** 14(2), 461.

[21]. Boettcher S. W. ; Oener, S.Z.; Lonergan, M.C.; Surendranath, Y.; Ardo, S.; Brozek, C.; Kempleret , P. A. *ACS Energy Letters* **2021,** 6, 261-266.

[22]. Bard A. J. and Faulkner L. R. Electrochemical methods : Fundamentals and Applications (John Wiley & Sons, INC. 2nd Edition, 2001).

[23]. Lewerenz H. J. On the Structure of the Helmholtz Layer and its Implications on Electrode Kinetics. *ECS Trans.* **2013,** 50 (52), 3-20.

[24]. Trasatti, S.; Lust, E.; The Potential of Zero Charge. Modern Aspects of Electrochemistry, Number 33, edited by Ralph E. White et al. Kluwer Academic / Plenum Publishers, New York, 1999.

[25]. Warren B.E. X-Ray diffraction (Dover Publications, 1990)

[26]. Templeton, D. H.; Templeton L. K. X-Ray dichroism an danomalous scattering of potessium tetrachloroplatinate(II). *Acta Crist. A* **1985,** 41, 365-371.

[27]. Le, J.-B.; Cheng, J. Modeling electrified metal/water interfaces from *ab initio* molecular dynamics: Structure and Helmholtz capacitance. *Curr. Opin. Electrochem.* **2021,** 27, 100693-100699.

[28]. Sebastián, P.; Martínez-Hincapié, R.; Climent, V.; Feliu, J.M. *Electrochim. Acta* **2017**, 228, 667–676.

[29]. Sakong, S.; Gross, A. The electric double layer at metal-water interfaces revisited based on a charge polarization scheme, *J. Chem. Phys.* **2018,** 149, 084705.

[30]. X-Ray Absorption, Principles, Applications, techniques of EXAFS, SEXAFS and XANES (ed. D.C. Koningsberger and R. Prins, Wiley, New York, 1988).

[31]. Schmickler, W.; Guidelli, R. The partial charge transfer. *Electrochim. Acta* **2014,** 127, 489–505.

TABLE OF CONTENTS GRAPHIC

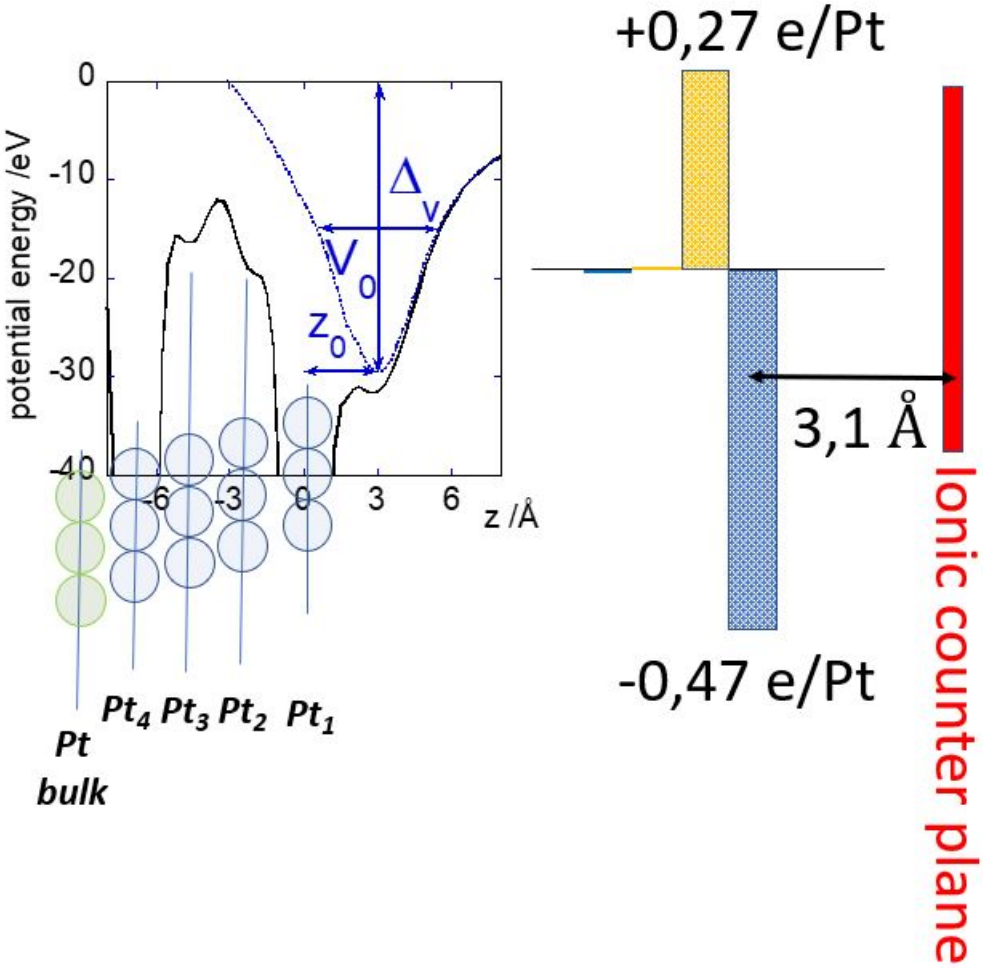

SUPPLEMENTARY INFORMATION

Unravelling the charge distribution at the metal-electrolyte interface coupling *in situ* surface resonant X-Ray diffraction with *ab initio* calculations

Yvonne Soldo-Olivier, Eric Sibert[#], Maurizio De Santis[^], Yves Joly[^] and Yvonne Gründer[§]*

*** Corresponding Author**

Yvonne Soldo-Olivier
CNRS, Université Grenoble Alpes, Institut Néel, 38042 Grenoble, France
yvonne.soldo@neel.cnrs.fr

Author information

[^] same address as the corresponding author

[#] Eric Sibert
LEPMI, Univ. Grenoble Alpes, Univ. Savoie Mont Blanc, CNRS, Grenoble INP, St. Martin d'Hères, France

[§] Yvonne Gründer
Oliver Lodge Laboratory, Department of Physics, University of Liverpool, United Kingdom

SI.1 Electrochemical operation mode

Detailed description of the thin-film electrochemical cell used in the SRXRD *in situ* experiment and of the procedure followed to make the electrochemical experiments are given in [1]. We briefly remind here the main points.

- **Surface preparation of the Pt(111) electrode in 0.1 M H_2SO_4**

We used a platinum (111) single crystal with an orientation accuracy of about 0.1° and a diameter of ca. 10 mm. Before each experiment, the Pt(111) surface was flame annealed (H_2/air) and cooled down in a reducing atmosphere (Ar+H_2 10%), as described previously[2]. The Pt(111) crystal, protected with an ultrapure water drop, was then transferred to the home-made electrochemical PTFE cell, specifically dedicated to *in situ* diffraction experiments. Previous the transfer to the PTFE cell and before each SRXRD experiment, the quality and cleanliness of the surface were checked by cyclic voltammetry in 0.1 M H_2SO_4. using a PAR 273A potentiostat, as described in the following paragraph.

The saturated calomel electrode (SCE) was used as a reference. In the paper, the potential is expressed versus the reversible hydrogen electrode (RHE) potential (0 V_{SCE}=+0.298 V_{RHE}).

- **Voltammetry of the Pt(111) electrode in 0.1 M H_2SO_4**

Figure S1 shows the voltammogram recorded on the Pt(111) crystal in 0.1M H_2SO_4 in a glass cell with the hanging meniscus technique, before the transfer to the electrochemical cell used during the diffraction experiments. Different electrochemical processes are distinctive of a clean and well-ordered Pt(111) surface, as a function of the potential region:

Region (a) below +0.4 V_{RHE}: it is characterized by hydrogen adsorption/desorption (negative/positive current).

Region (b) above +0.4 V_{RHE}: also called “unusual state”, it has been associated to anion desorption/adsorption (probably (hydrogeno)-sulfate) on ordered Pt(111) surfaces[3].

The intensity of the **peak (c),** very sharp and with a very small associated charge, as well as that of **peak (d),** is related to the to the surface quality and to the presence of long-range ordered (111) areas[4]. Voltammograms made in the dedicated cell before each *in situ* SRXRD experiment present the same signatures.

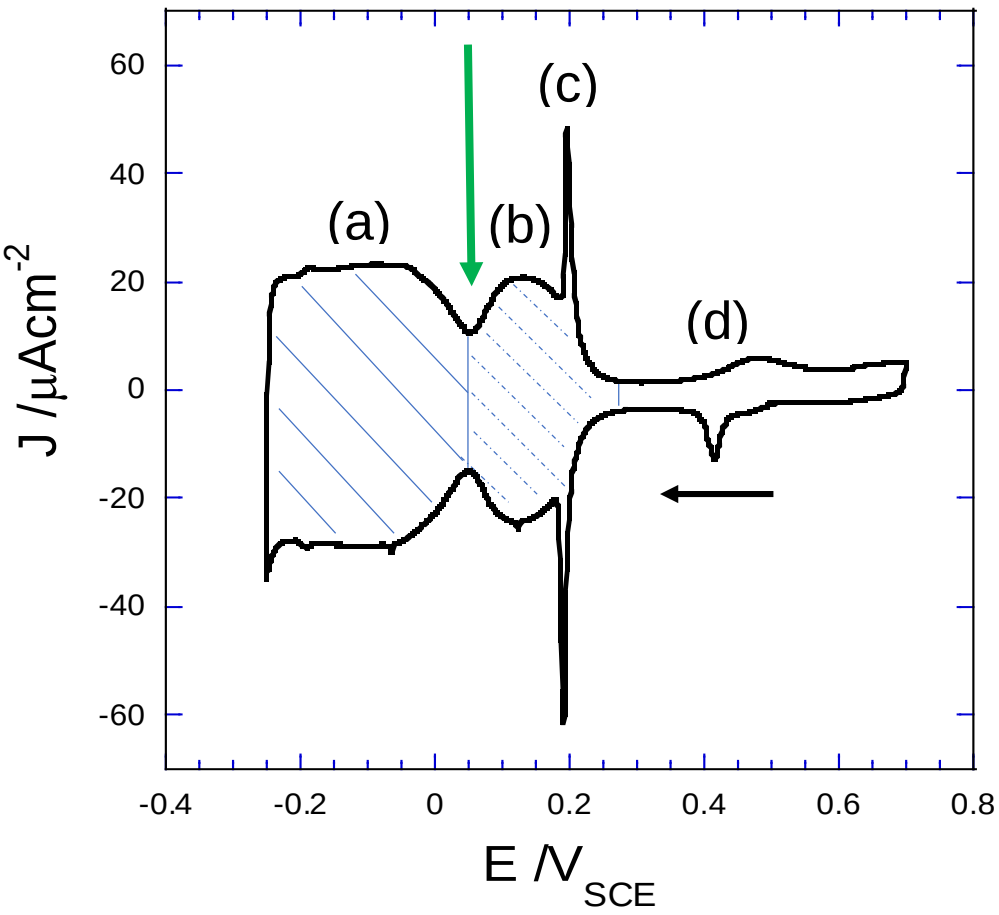

Figure S1: Voltammogram of Pt(111) in 0.1M H_2SO_4 (black line), 50mV/sec. Green arrow indicates the potential applied during our measurements, 0.050 $V_{SCE.}$

- **Electrochemical cell for *in situ* SRXRD experiments**

In situ SRXRD experiments were made in a dedicated electrochemical cell, allowing to work in grazing incidence in both σ and π polarization, while keeping the potential applied. Detailed scheme of the electrochemical cell is given in [1]. In front of the crystal surface, positioned on a piston in the center of the cell body, a polyethylene film allows an electrolyte thickness of only a few tens of micrometers in front of the crystal surface, minimizing the X-ray absorption by the solution. The Pt counter and auxiliary electrodes are installed through glass tubes in the cell next to the working electrode. The reference electrode, an usual saturated calomel electrode (SCE) in an external compartment, is linked to the cell by a PTFE tube. To avoid oxygen permeation through the polyethylene film, a kapton ® bell swept by a nitrogen flux is positioned on top of the cell.

SI.2 Experimental SRXRD operation mode

The SRXRD spectra were collected measuring the intensity while adjusting the diffractometer settings to keep (*H K L*) fixed during the energy scan. In surface x-ray diffraction experiments this is called the stationary mode[5]. This procedure was adopted to get spectra with a sufficiently small energy step while maintaining the acquisition time compatible with the electrochemical cell life time and with the available beam time

The normalisation factor of each experimental spectrum is the ratio between the integrals of the ab-initio and of the experimental data in the range [-40, 60] eV across the Pt L_{III}-edge edge. Prior to normalization, the background spectrum, recorded detuning the azimuthal angle outside the rocking curve width, was subtracted and Lorentz correction was applied. The correction due to the energy dependent X-ray absorption by the electrolyte was not applied, as we did not exactly determine the thickness of the liquid in front of the crystal; however, it is expected to be negligible over the small (100 eV) energy interval of the spectra.

SI.3 Fitting of the (0 1 L) CTR with ROD package

A portion of the (01) CTR was measured at fixed energy for structural analysis. The intensity was collected at different L values along the rod by integrating the signal during a rocking scan (crystal rotation around the direction normal to the surface). The modulus of the structure factor was then extracted by the integrated intensity after applying standard correction factors related to the diffractometer geometry[6]. Structural parameters optimization was performed with the ROD package [7], employing a χ^2 minimization for the refinement.

They are in very good agreement with previous *in situ* SXRD measurements on Pt(111) in 0.05MH_2S0_4 in the same potential region, showing an expansion of the last surface plane by 1.8% [8]and 2.2%[9] compared to Pt(111) bulk value and a surface layer occupation slightly smaller than one.

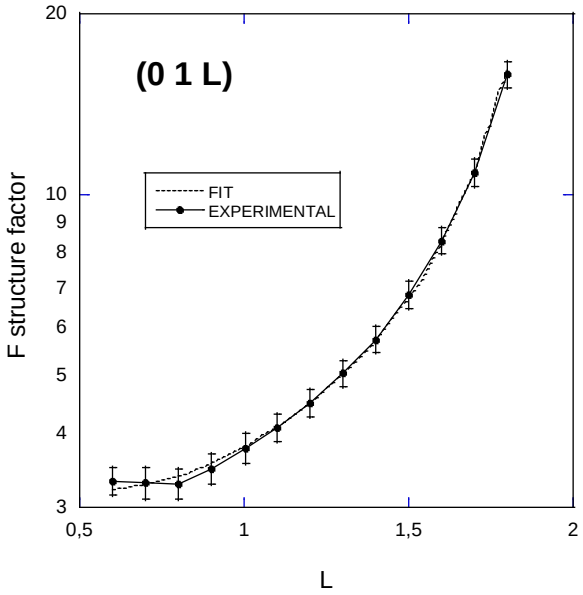

Figure S2. Pt(111) in H_2S0_4 0.1M at 350 mV_{RHE}: structure factor extracted from the experimental CTR (0 1 L) data recorded at 11568 eV in σ polarization after standard corrections and best fit signal obtained with ROD package (dotted line).

SI.4 *Ab initio* calculation

FDMNES works in direct space. It can operate using the multiple scattering theory with a muffin-tin approximation on the potential shape (spherically averaged in the atoms and constant between them) or within the Finite Difference Method (FDM), which is a free-shape potential, whose details are given in reference [10].

We used FDM because the presence of the surface makes the muffin-tin approximation rather poor, and more importantly, because the Helmholtz potential is otherwise difficult to be precisely described. Calculations are made in the fundamental state. As excited states probed by the photoelectron are slightly shifted in energy, an empirical parameter is used to take into account for that. One calculation is performed per each non-equivalent absorbing atom. In the present case, calculations are made with four surface layers plus the bulk. There are thus five inequivalent Pt atoms (all the atoms in the same plane are equivalent) and consequently five independent calculations. From these last, the five resonant scattering amplitudes are calculated in dipolar approximation following the equation:

$$f'(\omega) - if''(\omega) = m_e \sum_{E_n > E_F} \left(\frac{E_n - E_g}{\hbar}\right)^2 \frac{\sum_{n,g} \langle \varphi_g | \boldsymbol{\epsilon_s^*} \cdot \boldsymbol{r} | \varphi_n \rangle \langle \varphi_n | \boldsymbol{\epsilon_i} \cdot \boldsymbol{r} | \varphi_g \rangle}{\hbar\omega - (E_n - E_g) + i\frac{\Gamma}{2}} \quad \text{(SI.1)}$$

In the formula φ_n and φ_g are respectively the intermediate states above the Fermi energy E_F and the core states. E_n and E_g are their energies, ħω is the incident photon energy, m_e is the electron mass. $\boldsymbol{\epsilon_{i(s)}}$ are the incoming (outgoing) polarization and $\boldsymbol{r}$ stands for the position. It has been checked that the quadrupolar contribution is negligible at the studied edge.

The total structure factor for each atom is obtained adding the non-resonant Thomson contributions, f_{0a}

$$F_S(\boldsymbol{Q}, \omega) = \sum_a t_a e^{-i\boldsymbol{Q}.\boldsymbol{R_a}} \left(f_{0a} + f_a'(\omega) - if_a''(\omega)\right) \quad \text{(SI.2)}$$

where a index the atoms in the surface unit cell, $\boldsymbol{R_a}$ is the atom position and $\boldsymbol{Q} = H\boldsymbol{a}^* + K\boldsymbol{b}^* + L\boldsymbol{c}^*$ is the diffraction vector. $t_a$is the site occupancy multiplied by a Debye-Waller attenuation term.

Summing with the bulk contribution, F_B, one finally obtains the diffracted intensity [11]:

$$I(\boldsymbol{Q},\omega) \propto |F_S(\boldsymbol{Q},\omega) + F_B(\boldsymbol{Q},\omega)|^2 \qquad \text{(SI.3)}$$

For each of the five simulations, the volume of the calculation to get the φ_n is centered on the absorbing atom up to a sphere with a chosen radius. This one is increased up to convergence in term of spectra shape, reached at 7 Å for this material.

Beside the agreement between theory and experiment, an important criterion to check the validity of the self-consistency and of the model is that the five calculations must give coherent electronic structures and Fermi levels.

Technical details

Following previous tests, the calculations have been made with a non-excited absorbing atom.

The fitting procedure minimizing the total metric distance D value gives also the energy shift, the same for all the reflections, applied to the simulations to compare them to the experimental spectra, not exciding 1 eV.

SI.5 Confidence factor

Each calculated spectrum $I^i_{th}(E)$ is compared to the corresponding experimental one $I^i_{exp}(E)$ using the metric distance D_i defined as

$$D_i = \frac{1}{2}\int_{Emin}^{Emax} \left| \frac{1}{c^i_{th}} I^i_{th}(E) - \frac{1}{c^i_{exp}} I^i_{exp}(E) \right| dE$$

where c_i are the normalization factors

$$c_i = \int_{Emin}^{Emax} I^i(E)dE$$

Note that D_i is given in percent**.** The E_{min} and E_{max} values have been set equal to 40 eV before the Pt_{LIII} edge and 60 eV after the edge, respectively.

Experiments and simulations were compared using the total metric distance D obtained as the sum of all the individual D_i divided by the number of experimental spectra, as it has been used for many years in bulk resonant spectroscopy[12].

The error bars of V_0 and Ch_i correspond to a D value deviation of 2% from its minimum. This procedure has been followed referring to the method based on the D factor largely used in the spectroscopic technique LEED[13], as it presents large similarities with SRXRD both from the numerical and from the experimental point of view. This choice has already been previously used in resonant X-Ray diffraction experiments[14,15].

SI.6 Sensitivity of SRXRD spectra for the Pt2-Pt1 interplanar distance

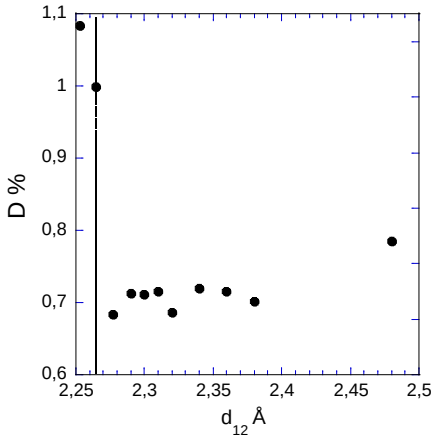

Figure S3: Total metric distance obtained from FDMNES calculations with Helmholtz potential (V_0=-30 eV, z_0=3 Å, Δ_V=5 Å, Ch=-0.20) as a function of the interlayer distance d_{12} between the two outermost surface Pt layers. The dotted vertical line indicates the bulk interplanar distance.

The D parameter behavior (figure S3) clearly shows that the last layer is expanded. Nevertheless, the expansion value cannot be determined with a good precision: D values are quite stable up to an expansion of about 6% (2.40 Å).

References

1. Soldo Y., Sibert E., Tourillon G., Hazemann J.L., Levy J.P., Aberdam D., Faure R., Durand R., *Electrochim. Acta* **2002,** 47, 3081-3091.

2. Soldo-Olivier Y. et al. Hydrogen Electro-Insertion into Pd/Pt(111) Nanofilms: An in *situ* Surface X-ray Diffraction Study. *J. Phys. Chem. C* **2011,** 115, 12041–12047

3. J.M. Feliu, J.M. Orts, R. Gómez, A. Aldaz, J. Clavilier, *Journal of Electroanalytical Chemistry*, **1994,** 372, 26

4. Nuria Garcia-Araez, V. Climent, P. Rodriguez and J. Feliu, *Electrochim. Acta* 53 (2008) 6793-6806

5. Torelles J. and Rius J. Faster acquisition of structure-factor amplitudes in Surface X-Ray Diffraction experiments. *J. Appl. Cryst*. **2004,** 37, 395-398

6. Vlieg, E. J. Integrated Intensities Using a Six-Circle Surface X-ray Diffractometer. *Appl. Cryst.* **1997,** 30, 532-543.

7. Vlieg, E. J. ROD: a program for surface X-ray crystallography. *Appl. Cryst*. **2000,** 33, 401-405.

8. Kondo T., Masuda T., Aoki N., and Uosaki K., Potential-Dependent Structures and Potential-Induced Structure Changes at Pt(111) Single-Crystal Electrode/Sulfuric and Perchloric Acid Interfaces in the Potential Region between Hydrogen Underpotential Deposition and Surface Oxide Formation by *in situ* Surface X-ray Scattering. *J. Phys. Chem. C* **2016,** 120, 16118−16131.

9. Tidswell I. M.; Markovic, N. M.; Ross, P. N. Potential Dependent Surface Structure of the Pt(111)|Electrolyte Interface. *J.Electroanal. Chem.* **1994,** 376, 119−126.

10. Joly Y. Finite-difference method for the calculation of low-energy-electron diffraction, *Phys. Rev. Lett.* **1992**, 68, 950-953.

11 Joly Y. et al. Simulation of Surface Resonant X-ray Diffraction. *Journal of Chemical Theory and Computation* **2018**, 14(2), 973–980.

12. Joly Y. et al. Low-temperature structure of magnetite studied using resonant x-ray scattering. *Physical Review B* **2008,** 78, 134110.

13. Philip J. and Rundgren J. Proceedings of the Conference on Determination of Surface Structure by LEED (Yorktown Heights, 1980, edited by P. M. Marcus, Plenum, New York, 1984)

14 Nazarenko E. et al. Resonant X-Ray Diffraction Studies on the Charge Ordering in Magnetite. *Physical Review Letter* **2006,** 97, 056403.

15. De Santis M. et al. Epitaxial growth and structure of cobalt ferrite thin films with large inversion parameter on Ag(001), *Acta Cryst.* **2019,** B75, 8–17.